



## Removal of lead(II) from water by di (2-ethylhexyl) phosphate containing ion exchange resin

Özgür Arar

Faculty of Science, Department of Chemistry, Ege University, 35100 Izmir, Turkey  
Tel. +90 232 3112389; Fax: +90 232 3888264; email: ozgur.arar@ege.edu.tr

Received 31 January 2013; Accepted 16 April 2013

---

### ABSTRACT

In the present study, commercially available chelating resin with the di (2-ethylhexyl) phosphate functional group (Lewatit VP OC 1026) has been evaluated for its suitability for the removal of  $Pb^{2+}$  from water. Studies for the removal of  $Pb^{2+}$  in different resin doses, pH of the solution, adsorption mechanism, and kinetic performance of resin were carried out. The obtained results showed that the removal performance of resin strongly depends on solution pH. More than 99% removal of  $Pb^{2+}$  was achieved at  $pH \geq 3$ . The experimental equilibrium data were tested for the Langmuir and Freundlich isotherms. Correlation coefficients indicate that the Langmuir isotherm fits better than the Freundlich isotherm. Pseudo-first- and -second-order kinetic models were used to describe kinetic data. It was determined that the removal of  $Pb^{2+}$  well-fitted by second-order reaction kinetics.

*Keywords:* Di (2-ethylhexyl) phosphate; Ion exchange; Kinetic models; Lead; Lewatit VP OC 1026

---

### 1. Introduction

Lead (Pb) is ubiquitous and one of the earliest metals to have been discovered by the human race. The unique properties of lead, like softness, high malleability, ductility, low melting point, and resistance to corrosion have resulted in its widespread usage in different industries like automobiles, paint, ceramics, plastics, and so on. This in turn has led to a manifold rise in the occurrence of free lead in biological systems and the inert environment [1]. The vast increase in environmental lead has dramatically raised the measured blood concentration of lead in many people. Lead causes severe health effects even at relatively low levels in the body, including often irreversible brain damage and injury to the blood forming systems.

At the typical levels to which individuals are exposed, lead can cross the placenta and damage developing fetal nervous systems [2]. Lead is present in tap water to some extent as a result of its dissolution from natural sources, but primarily from household plumbing systems in which the pipes, soldered joints, fittings, or service connections to homes contain lead. Polyvinyl chloride pipes also contain lead compounds that can be leached from them and result in high lead concentrations in drinking water. The amount of lead dissolved from the plumbing system depends on several factors, including the presence of chloride and dissolved oxygen, pH, temperature, water softness, and standing time of the water; soft, acidic water being the most plumb solvent. Although lead can be leached from lead piping indefinitely, it

appears that the leaching of lead from soldered joints and brass taps decreases with time [3].

The processes that have been developed to remove lead from wastewater include biosorption [4–7], electro-membrane processes [8,9], adsorption [10–13], coagulation–flocculation [14], and ion exchange [15–17].

At low-solute feed concentrations, the use of solvent extraction or solvent-based membrane processes loses their advantage. Often under these conditions, the loss of solvent into the aqueous wastewater phase through solubility or entrainment is greater than the quantity of solute recovered. In this instance, an alternative technology is required. The use of a solid matrix for adsorption and ion exchange of contaminants provides such an alternative. Ion exchange is a proven technique for the purification and separation of metals from aqueous solutions using solid ion exchange resins. The process is effective particularly for the removal of metallic ions from the dilute solutions (<0.5 g/l) where precipitation is not efficient [18]. The advantages of Lewatit VP OC 1026 to solvent extraction are; organic solvent is not required, there is no phase separation problem, and simple equipment required for separation. Cortina et al. studied the extraction studies of Zn(II), Cu(II), and Cd(II) (II) from nitrate and chloride solution by Lewatit VP OC 1026 resin [19].

In this study, the removal of  $Pb^{2+}$  from water by di (2-ethylhexyl) phosphate (D2EHPA) containing ion exchange resins was carried out. The effects of the resin amount and solution pH on the removal of  $Pb^{2+}$  were investigated. FTIR analysis of resin and  $Pb^{2+}$  loaded resin was compared.

## 2. Experimental

### 2.1. Materials

Lewatit VP OC 1026 was kindly provided by Lanxess-Lewatit company. The physicochemical characteristics of resin are summarized in Table 1.

Table 1  
Physical and chemical properties of resin

Functional group	D2EHPA
Matrix	Crosslinked polystyrene
Structure	Macroporous
Operating pH-range	1–6
Operating temperature (°C)	Max 80
Density approx. (g/mL)	0.97
Specific gravity	1.08

### 2.2. Preparation of solution

The stock  $Pb^{2+}$  solution (1,000 mg  $Pb^{2+}$ /L) was prepared with  $Pb(NO_3)_2$  dried at 110°C. About 1.5981 g of  $Pb(NO_3)_2$  was dissolved in water containing 1 mL of concentrate  $HNO_3$  (14M) and diluted to 1.0 L with pure water. The working  $Pb^{2+}$  solution was prepared by dilution of stock solution. The pH of the solution was adjusted with NaOH or  $HNO_3$ . All chemicals were analytical grade.

### 2.3. Batch-mode sorption studies

#### 2.3.1. Optimum resin amount

In this series of experiments, the optimum resin dosage was determined using various amounts of the resin (0.010, 0.025; 0.05; 0.075 0.10; 0.20; and 0.30) in contact with 25 mL of  $Pb^{2+}$  solution (20 mg  $Pb^{2+}$ /L, pH 4) equilibrated for 24 h at 25°C with continuous shaking. After 24 h, the aqueous phase was separated from resins and the concentrations of the  $Pb^{2+}$  in the aqueous phase were determined using an atomic absorption spectrometer (Varian SpectrAA 220 model) at a wavelength of 217.0 nm. The standard deviation of each measurement is <1.0% (Each sample analyzed three times)

#### 2.3.2. Optimum pH

In order to find the optimum pH, 0.075 g (the optimum amount) of the resins was added to 25 mL 20 mg  $Pb^{2+}$ /L solution at various pH in the 1–5 range equilibrated for 24 h at 25°C with continuous shaking. After 24 h, the aqueous phase was separated and the  $Pb^{2+}$  concentration in the solution was analyzed.

#### 2.3.3. Equilibrium adsorption isotherm

For equilibrium adsorption isotherm, 0.075 g of the resins was in contact with 25 mL  $Pb^{2+}$  solution with concentrations of 50, 75, 100, 125, 150, and 200 mg/L (pH 4) at 25°C for 24 h under continuous shaking. After 24 h, the aqueous phase was separated from resins and the  $Pb^{2+}$  concentration in the solution was analyzed (after adequate dilution).

#### 2.3.4. Kinetic experiments

Batch kinetic tests were performed by contacting 3.0 g of resin with 1.0 L of  $Pb^{2+}$  solution (20 mg/L at pH 4). The solution was stirred with an overhead mixer.  $Pb^{2+}$  concentrations were monitored by taking samples at prescribed times (1, 3, 5, 10, 15, 30, 45, 60, 90, 120, 180, 240, and 300 min).

### 2.4. FTIR analysis

Fourier transformed infrared spectroscopy was performed with a Perkin–Elmer FTIR Spectrum One-B spectrometer. For qualitative analysis, 1 mg of the sample per 100 mg of KBr was employed.

## 3. Results and discussion

### 3.1. Effect of resin dose on Pb<sup>2+</sup> removal

To find an appropriate resin amount for the complete removal of Pb<sup>2+</sup> from aqueous solution, a batch-mode sorption study was performed by varying the dose of resins. Fig. 1 shows the removal of Pb<sup>2+</sup> as a function of resin dose. The adsorption capacity ( $q_e$ , mg/g) and the removal percentage ( $A$ , %) were calculated from the following equations [20]:

$$q_e = V \frac{C_0 - C_e}{m_s} \quad (1)$$

$$A = \frac{C_0 - C_e}{C_0} \times 100 \quad (2)$$

where  $C_0$  and  $C_e$  (mg/L) are the initial and final concentrations of Pb<sup>2+</sup> in the solution,  $V$  is the volume of the solution (L), and  $m_s$  is the mass of dry resin (g).

The percent removal of Pb<sup>2+</sup> increased with increasing sorbent concentration. This result was expected because for a fixed initial metal concentration, increasing adsorbent amount provides greater ion exchange sites [21,22]. As can be seen from Fig. 1, the optimum resin dose was found to be 0.075 g/25 mL of solution (i.e. 3 g resin/L).

### 3.2. Effect of pH

It is well known that the pH of the solution is an important variable in the ion exchange process. To

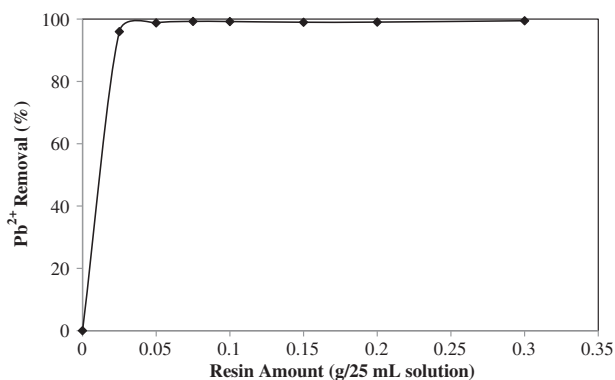


Fig. 1. Effect of resin amount on removal of Pb<sup>2+</sup> ion from aqueous solution.

identify the dependency of the ion exchange process, the model solution pH values varied from 1 to 5 by using HNO<sub>3</sub> or NaOH. The 25 mL of Pb<sup>2+</sup> solution (20 mg/L) was in contact with 0.075 g resin. Fig. 2 shows the effect of pH on the removal of Pb<sup>2+</sup> from solution.

As can be seen from Fig. 2, when the pH of the solution was increased, the percent removal of Pb<sup>2+</sup> increased and over pH ≥ 3, more than 99% removal of Pb<sup>2+</sup> was obtained. This can be explained as follows; the pKa value of D2EHPA is reported as 1.9 in the aqueous solution at 25°C [23]. Therefore, when the pH was increased, the H<sup>+</sup> are displaced from the functional group of the resin, thus allowing the ion exchange of the Pb<sup>2+</sup> to the resin [24].

### 3.3. Adsorption isotherm

The most commonly used equations for modeling sorption equilibrium data are the Langmuir and Freundlich isotherms.

#### 3.3.1. Langmuir model

The Langmuir isotherm is a commonly applied model for adsorption on a completely homogenous surface with negligible interaction between adsorbed molecules. The model assumes uniform adsorption energies onto the surface and maximum adsorption depends on the saturation level of the monolayer [25]. The Langmuir model can be represented with the following linear equation:

$$\frac{C_e}{Q_e} = \frac{1}{bQ_0} + \frac{C_e}{Q_0} \quad (3)$$

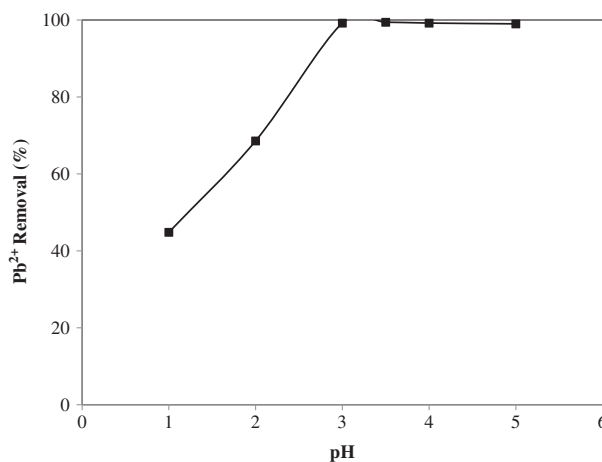


Fig. 2. Effect of pH on the removal of Pb<sup>2+</sup>.

where  $Q_e$  (mg/g) is the amount of  $Pb^{2+}$  adsorbed per gram of dry resin at equilibrium,  $C_e$  is the equilibrium concentration of  $Pb^{2+}$  in the solution (mg/L),  $Q_0$  (mg/g), and  $b$  (L/mg) are the Langmuir constants related to the capacity and energy of sorption, respectively.

### 3.3.2. Freundlich model

The Freundlich model is known as the earliest empirical equation and is shown to be consistent with exponential distribution of active centers, characteristic of heterogeneous surfaces [26]. The Freundlich equation is:

$$\log Q_e = \log K_f + \frac{1}{n} \log C_e \quad (4)$$

where  $K_f$  and  $n$  are the Freundlich constants that indicate relative capacity and adsorption intensity, respectively.

The equilibrium data for the sorption of  $Pb^{2+}$  from aqueous solution by VP OC 1026 resin at an initial pH of 4 was determined at an increasing initial concentration of  $Pb^{2+}$  (50–200 mg  $Pb^{2+}$ /L) until the saturation of resin. The maximum capacity of resin was found to be 35.6 mg  $Pb^{2+}$ /g resin. The experimental data of the ion-exchange equilibrium for the sorption of  $Pb^{2+}$  on the resin and also the fitting of the experimental data with the Langmuir and Freundlich isotherms ( $q_e$  vs.  $C_e$ ) is depicted in Fig. 3, the correlation coefficient for the linear regression fit of the Langmuir and Freundlich isotherms and their constants are summarized in Table 2.

The plot of  $Pb^{2+}$  uptake against equilibrium concentration indicates that adsorption increases initially with concentration but then reaches saturation. The decrease in the curvature of the isotherm, at it tends to a monolayer, as the  $C_e$  values increase considerably for a small increase in  $q_e$ , is possibly due to the less active sites being available at the end of the adsorption process and/or the difficulty of the edge solutes in penetrating the adsorbent, lead-ions partially covering the surface sites of resin [13].

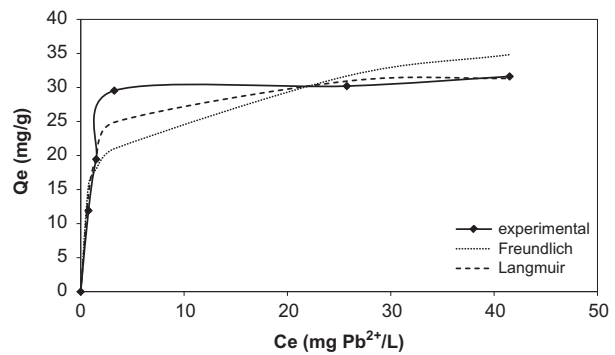


Fig. 3. Equilibrium isotherms of  $Pb^{2+}$  on Lewatit VP OC 1026 resin.

The  $R^2$  values in Table 2 suggested that the Langmuir isotherm provides a good model of the sorption system. The sorption capacity,  $Q_0$ , found 35.59 mg/g for Lewatit resin. The adsorption coefficient,  $b$ , which is related to the apparent energy of adsorption for  $Pb^{2+}$  found as 0.457 L/mg.

The shape of the Langmuir isotherm can be used to predict whether a sorption system is favorable or unfavorable in a batch adsorption process. Accordingly, the essential features of the Langmuir isotherm was expressed in terms of a dimensionless constant called the equilibrium parameter,  $E_p$ , which is defined by the following relationship [27]:

$$E_p = \frac{1}{1 + bC_0} \quad (5)$$

where  $E_p$  is a dimensionless equilibrium parameter or separation factor;  $b$  = constant from Langmuir equation; and  $C_0$  = initial metal ion concentration.

The parameter,  $E_p$ , indicates the shape of the isotherm and nature of the sorption process as given; if  $E_p > 1$  Unfavorable isotherm,  $E_p = 1$  Linear isotherm,  $E_p = 0$  Irreversible Isotherm, and if  $0 < E_p < 1$  Favorable isotherm. [27].

In all worked concentration  $E_p$  values was higher than 0 and lower than 1. Obtained results show that sorption of  $Pb^{2+}$  by Lewatit resin is favorable.

Table 2  
Isotherm constants for  $Pb^{2+}$  sorption by ion exchange resin

Resin	Langmuir isotherm constants			Freundlich isotherm constants		
	$Q_0$ (mg/g)	$b$ (L/mg)	$R^2$	$K_f$ (mg/g)	$n$	$R^2$
Lewatit VP OC 1026	35.59	0.457	0.99	14.87	4.81	0.92

### 3.4. Kinetic tests and modeling

To have an idea about the kinetic performance of Lewatit VP OC 1026 resin, Pb<sup>2+</sup> uptake was monitored with time and experimental data were evaluated using the pseudo-first-order and pseudo-second-order kinetic models.

Fig. 4 shows the removal of Pb<sup>2+</sup> vs. time for Lewatit VP OC 1026 resin. As shown in Fig. 4, the removal of Pb<sup>2+</sup> is fast. More than 99% of Pb<sup>2+</sup> was removed in 45 min.

In order to predict the mechanism involved in the sorption process, Lagergren pseudo-first- and pseudo-second-order models were used.

The sorption kinetics following the pseudo-first-order model are given by [28]

$$\frac{dq}{dt} = k_1(q_e - q_t) \tag{6}$$

where  $q_e$  and  $q_t$  represent the amount of adsorbed species (mg/g) at equilibrium time and at any time  $t$ , respectively, and  $k_1$  represents the sorption rate constant (min<sup>-1</sup>) integrating Eq. (6) with respect to the boundary conditions

$q_t = 0$  at  $t = 0$  and  $q_t = q_t$  at  $t = t$ , one obtains

$$\log(q_e - q_t) = \log(q_e) - \frac{k_1 t}{2.303} \tag{7}$$

The sorption rate constant  $k_1$  (min<sup>-1</sup>) can be calculated from the plot of  $\log(q_e - q_t)$  vs. time.

The pseudo-second-order model is presented by the following equation [28]

$$\frac{dq}{dt} = k_2(q_e - q_t)^2 \tag{8}$$

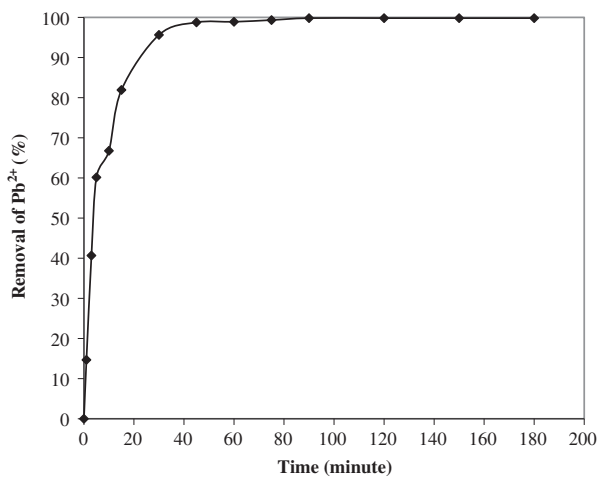


Fig. 4. Removal of Pb<sup>2+</sup> vs. time.

where  $k_2$  is the pseudo-second-order rate constant (g/mg min),  $q_e$  and  $q_t$  are the amounts of adsorbed species (mg/g) at equilibrium and at time  $t$ . Varying the variables in Eq. (8), one gets

$$\frac{dq}{(q_e - q_t)^2} = k_2 dt \tag{9}$$

$t = 0$  to  $t = t$  and  $q = 0$  and  $q = q_e$  one obtains the final form

$$\frac{t}{q_t} = \frac{1}{k_2 q_e^2} + \frac{1}{q_e} t \tag{10}$$

A plot  $t/q$  vs.  $t$  gives the value of the constants  $k_2$  (g/mg min). It is also possible to calculate  $q_e$  (mg/g). The constant  $k_2$  is used to calculate the initial sorption rate  $r$  at  $t \rightarrow 0$ , as follows [13,29]:

$$r = k_2 q_e^2 \tag{11}$$

If a pseudo-second-order kinetics model is applicable, the plot of  $t/q_t$  against  $t$  should give a linear relationship, which  $q_e$ ,  $k$  can be determined from the slope and intercept of the plot and there is no need to know any parameter beforehand. The calculated parameter of pseudo-first- and second-order kinetic model was summarized in Table 3.

As shown in Figs. 5 and 6 when the linear correlation coefficients were compared, it was seen that the sorption kinetics for resin agreed well with the pseudo-second-order mechanism.

Batch kinetic runs were evaluated using some mathematical models. The infinite solution volume models (ISV) and the unreacted core models (UCM) were also examined for the relative kinetic performance and to investigate the sorption mechanism. In the ISV Models, the rate determining step is normally described by either the diffusion of ions through the liquid film surrounding the particle, film diffusion, or

Table 3  
The calculated parameters of pseudo first and pseudo second order kinetic model

Kinetic model	Parameter	Value
Pseudo-first-order	$k_1$ (min <sup>-1</sup> )	0.08
	$q_e$ (mg/g)	4.69
	$R^2$	0.96
Pseudo-second-order	$k_2$ (g/mg min)	0.01
	$q_e$ (mg/g)	18.94
	$r$ (mg/g min)	3.62
	$R^2$	0.99

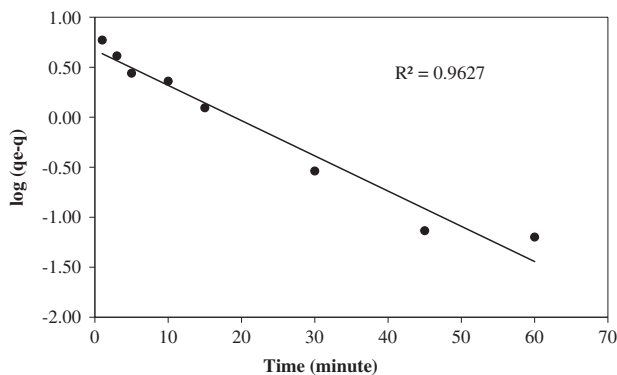


Fig. 5. Pseudo-first-order reaction kinetics for the adsorption of  $Pb^{2+}$  onto Lewatit VP OC 1026 resin (calculated  $k_1 = 0.0811 \text{ min}^{-1}$ ).

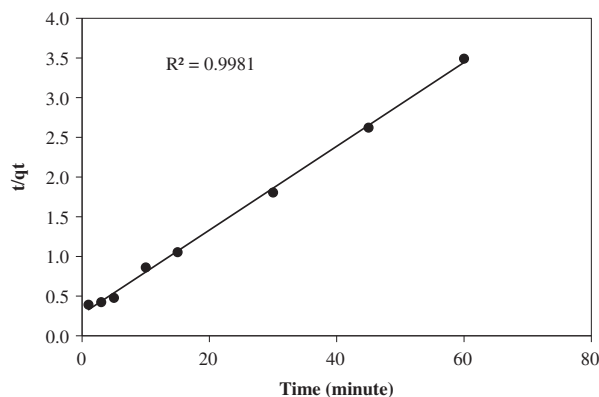


Fig. 6. Pseudo-second order reaction kinetics for the adsorption of  $Pb^{2+}$  onto Lewatit VP OC 1026 (calculated  $k_2 = 0.0101 \text{ g/mg min}$ ).

the diffusion of ions into the sorbent beads, particle diffusion [30–31].

$$F(X) = -\ln(1 - X) = k_{it} \quad (12)$$

If the film diffusion is the rate controlling mechanism a straight line should be obtained by plotting  $\ln(1 - X)$  against time,  $t$ . The slope is given by the expression  $3DC/r_o\delta Cr$ .

If the diffusion of ions through the resin beads is the slowest step, particle diffusion will be rate-determining and the particle diffusion model can be applied to calculate the diffusion coefficient. Then, the rate equation is expressed by Eq. (13):

$$F(X) = -\ln(1 - X^2) = 2kt \quad (13)$$

In the case of the particle diffusion is in control of the ion exchange mechanism, the extent of the resin

conversion  $\ln(1 - X^2)$  plotted against  $t$  should produce a straight line and its slope is given by the expression  $D_r\pi^2/r_o^2$ .

When the porosity of the polymer is small and thus is practically impervious to the fluid reactant, the reaction may be explained by the UCM approach. The kinetic concept of this mechanism can be described in terms of the concentration profile of a liquid reactant containing a counterion A advancing into a spherical bead of a partially substituted ion exchanger. As the reaction progresses in the bead, the material balances of counterion A follows Fick's diffusion equation with spherical coordinates. In this case, the relationship between reaction time and degree of conversion is given by the following expressions [30,31].

(a) with fluid film control:

$$F(X) = X = kt \quad (14)$$

In the case of the film diffusion is in control of the ion exchange mechanism, the extent of the resin conversion  $X$ , plotted against  $t$  should produce a straight line and its slope is given by the expression  $3C_{Ao}K_{MA}/ar_oC_{So}$ .

(b) with control by diffusion through the reacted layer:

$$F(X) = [3 - 3(1 - X)^{2/3} - 2X] = kt \quad (15)$$

Then, a plot of  $[3 - 3(1 - X)^{2/3} - 2X]$  against  $t$  should produce a straight line and its slope is given by the expression  $6D_{eR}C_{Ao}/ar_o^2 C_{So}$ .

(c) with chemical reaction control:

$$F(X) = [1 - (1 - X)^{1/3}] = kt \quad (16)$$

In the case of the slowest step is the chemical reaction, the extent of the resin conversion  $[1 - (1 - X)^{1/3}]$  plotted against  $t$  should produce a straight line and its slope is given by the expression  $K_sC_{Ao}/r_o$ .

For the evaluation of the kinetic models, only data from the first 60 min of the process was analyzed as then the resin reached equilibrium and data after this time was neglected. The results of linear regression analysis for both functions are summarized in Table 4. Linear correlation coefficients of five models for  $Pb^{2+}$  adsorption help to decide the rate-determining step. According to the ISV models, one can conclude that the  $Pb^{2+}$  adsorption onto the resin is a film diffusion-controlled process. As summarized in Table 4, the highest correlation coefficient was also found for the reacted layer step using UCM.

Table 4  
Linear regression analysis data related to diffusion models on sorption kinetics of Pb<sup>2+</sup> from water resin

Method	Equation	<i>k</i>	Rate-controlling step	R <sup>2</sup> value
ISV	$-\ln(1-X) = k_{it}t$	$k = 3DC/r_o\delta C_r$	Film diffusion	0.99
	$-\ln(1-X^2) = kt$	$k = Dr\pi^2/r_o^2$	Particle diffusion	0.97
UCM	$X$	$k = 3C_{Ao}K_{MA}/ar_oC_{So}$	Liquid film	0.72
	$3-3(1-X)^{2/3}-2X = kt$	$k = 6D_{eR}C_{Ao}/ar_o^2 C_{So}$	Reacted layer	0.97
	$1-(1-X)^{1/3} = kt$	$k = K_sC_{Ao}/r_o$	Chemical reaction	0.94

### 3.5. FTIR analysis

The FTIR spectrum of Lewatit VP OC 1026 resin before and after contacting with Pb<sup>2+</sup> was recorded and was shown in Fig. 7. IR absorption frequencies assignments for the polymeric matrix and D2EHPA molecules are given in Table 5. The spectrum associated with the polymeric matrix of styrene/divinyl benzene exhibits four strong bands at 3,027, 2,961, 2,929, and 2,867 cm<sup>-1</sup>, ascribed to the stretching modes of the aromatic and aliphatic C-H groups [19]. The FTIR spectra of D2EHPA have been analyzed and results are quite similar to those found by literature [19,32–34]. The P–O–C group showed an intense absorption band around 1,030 cm<sup>-1</sup>. This group appears to have two stretching frequencies, one primarily due to the stretching of the P–O bond and the other due to the O–C stretching (904 and 830 cm<sup>-1</sup>).

The P=O stretching frequency has been assigned at 1,230 cm<sup>-1</sup> [19,35]. The interaction between Pb<sup>2+</sup> and D2EHPA species has been identified by two distinct IR vibrational bands as shown in Fig. 7: (a) 1,032 cm<sup>-1</sup>, related to P–O–C and P–O–H overlapped bonds, (b) 1,231 cm<sup>-1</sup>, related to P=O bond. The relative intensities of the bands at 1,232 and 1,032 cm<sup>-1</sup> decreased when Pb<sup>2+</sup> was adsorbed by resins.

The FTIR spectroscopic studies of the resin (before and after Pb<sup>2+</sup> adsorption) indicates a transmittance decrease in the phosphoryl group of the DEHPA molecules. This is because of the phosphoryl oxygen atom may have coordinative activity with Pb<sup>2+</sup>. These metal complexes involve coordination between the phosphoryl oxygen atom and the central ions, in addition to the ionic bonds between oxygen (P–O) and central ions. Thus, P–O bond transmittance also decreased.

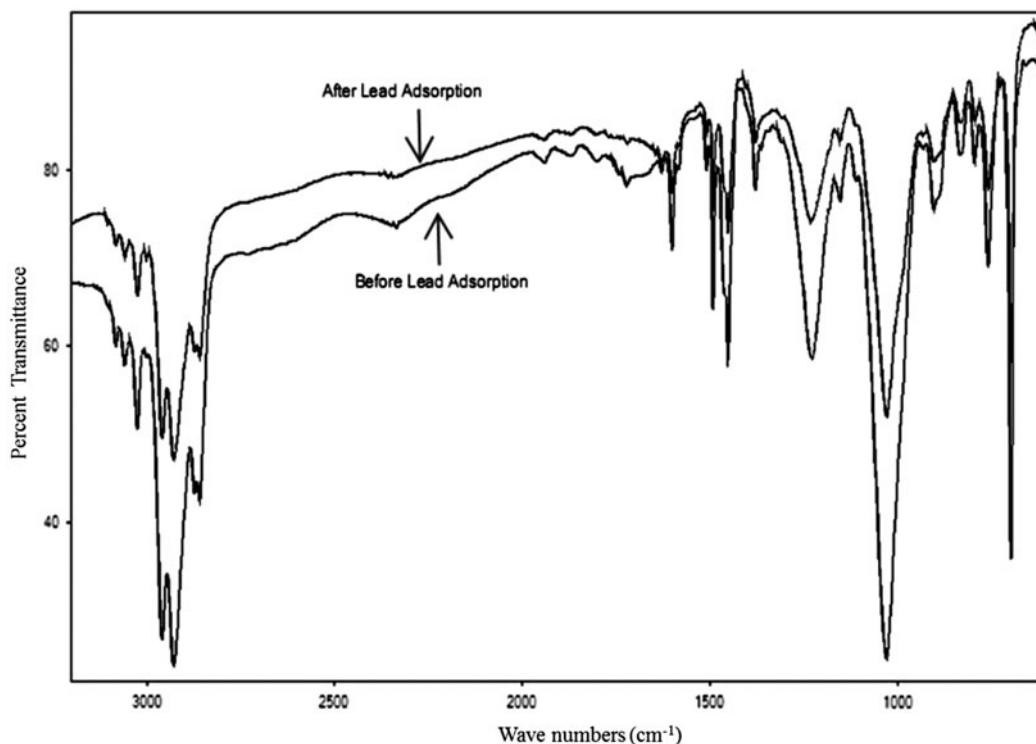


Fig. 7. FTIR spectra of Lewatit VP OC 1026 resin (before and after Pb<sup>2+</sup> adsorption).

Table 5  
Some main frequencies of Lewatit 1026 OC resin and Pb-D2EHPA complex

Frequency (cm <sup>-1</sup> )	Assignment
3,026	Aromatic C–H stretching
2,960	Aromatic C–H stretching
2,929	Aliphatic C–H stretching
2,861	Aliphatic C–H stretching
1,602	C=C ring stretching
1,493	C=C ring stretching
14,503	C=C ring stretching
1,231	P=O stretching
1,032	P–O–C stretching
906	P–O–C stretching
837	P–O–C stretching
699	C=C out of plane (flexion)

### 3.6. Regeneration of resin

Recovery of Pb<sup>2+</sup> from the resin was checked with hydrochloric acid and nitric acid solutions at different concentrations. Elution efficiency is calculated using the following Eq. (17)

Regeneration (elution) efficiency (%)

$$= \frac{\text{amount of eluted Pb}^{2+}(\text{mg})}{\text{amount of sorbed Pb}^{2+}(\text{mg})} \times 100 \quad (17)$$

As shown in Table 5, when the HNO<sub>3</sub> concentration was increased from 1.0 to 2.0M, the regeneration efficiency increased from 65% to 80%. HNO<sub>3</sub> solution has oxidation properties. In order to protect resin more concentrated HNO<sub>3</sub> solution was not used. In case of HCl, desorbed amount of Pb(II) increased by increasing of HCl concentration. When the 1.0M HCl was used for regeneration, 50% of Pb(II) desorbed in case of 4.0M HCl 70% of Pb<sup>2+</sup> desorbed from resin (Table 6).

Table 6  
Effect of acid concentration on desorption of Pb(II) from resin

Name of acid	Concentration (M)	Desorbed amount of Pb (%)
HCl	1.0	51
	2.0	55
	3.0	60
	4.0	70
HNO <sub>3</sub>	1.0	65
	2.0	80

## 4. Conclusion

In the present study, batch and kinetic tests for Pb<sup>2+</sup> removal from aqueous solution were conducted using Lewatit VP OC 1026 resin. Lewatit resin showed a great sorption performance for Pb<sup>2+</sup> removal from aqueous solution. The optimum resin amount for Pb<sup>2+</sup> removal from aqueous solution was found as 3.0 g resin/L. The obtained results show that the maximum capacity of resin is 35.6 mg Pb<sup>2+</sup>/g dry resin. The pH of the solution is important on Pb<sup>2+</sup> removal, when the pH of solution was increased the removal of Pb<sup>2+</sup> increased. The maximum removal of Pb<sup>2+</sup> was obtained at pH ≥ 3. The kinetic of the resin is very fast; more than 99% removal was achieved in 45 min. The kinetic data have been analyzed using pseudo-first- and- second-order equations. The characteristic parameters for each kinetic equation and related correlation coefficients have been determined. It was clear that the sorption kinetics of Pb<sup>2+</sup> to ion exchange resin obeyed second-order adsorption kinetics. The adsorption isotherms followed the Langmuir model. Pb<sup>2+</sup> loaded resin was eluted by using HNO<sub>3</sub> or HCl solution. About 80% of Pb<sup>2+</sup> desorbed from resin by using 2.0 M HNO<sub>3</sub>. When the 4.0 M HCl was used, 70% of Pb<sup>2+</sup> desorbed.

## Acknowledgments

I thank Lanxess - Lewatit and their distributor in Turkey; Ökotek Environmental Technologies and Chemical Industries for sending me resin. I would like to acknowledge Raif Ilktac and Tulin Deniz Ciftci for AAS analyses.

## Nomenclature

X	—	fractional attainment of equilibrium or extent of resin conversion
D	—	diffusion coefficient in solution phase (m <sup>2</sup> s <sup>-1</sup> )
C	—	total concentration of both exchanging species (M)
r <sub>o</sub>	—	average particle radius (mm)
δ	—	film thickness (mm)
Cr	—	total concentration of both exchanging species in the ion exchanger (M)
D <sub>r</sub>	—	particle diffusion coefficient in solid phase (m <sup>2</sup> s <sup>-1</sup> )
C <sub>Ao</sub>	—	concentration of species A in bulk solution (M)
K <sub>mA</sub>	—	mass transfer coefficient of species through the liquid film (m s <sup>-1</sup> )
C <sub>so</sub>	—	concentration of solid reactant at the bead's unreacted core (M)
a	—	stoichiometric coefficient
D <sub>er</sub>	—	effective diffusion coefficient in solid phase (m <sup>2</sup> s <sup>-1</sup> )
k <sub>s</sub>	—	reaction constant based on surface (m s <sup>-1</sup> )

## References

- [1] G. Flora, D. Gupta, A. Tiwari, Toxicity of lead: A review with recent updates, *Interdiscip. Toxicol.* 5 (2012) 47–58.
- [2] B. Yu, Y. Zhang, A. Shukla, S.S. Shukla, K.L. Dorris, The removal of heavy metals from aqueous solutions by sawdust adsorption—removal of lead and comparison of its adsorption with copper, *J. Hazard. Mater.* 84 (2001) 83–94.
- [3] WHO Guidelines for Drinking-water, Lead in Drinking-water Background Document for Development of, Quality World Health Organization, WHO Press, Geneva, 2011.
- [4] A.H. Sulaymon, S.E. Ebrahim, S.M. Abdullah, T.J. Al-Musawi, Removal of lead, cadmium, and mercury ions using biosorption, *Desalin. Water Treat.* 24 (2010) 344–352.
- [5] H. Yazid, L. Amour, A. Terkmani, R. Maachi, Biosorption of lead from aqueous solution by biologically activated date pedicels: batch and column study, *Desalin. Water Treat.* 51 (2013) 1690–1699.
- [6] Y. Chen, L. Ding, J. Nie, Isotherm and thermodynamic studies of the biosorption of lead, cadmium and copper from aqueous solutions by rice bran, *Desalin. Water Treat.* 44 (2012) 168–173A.
- [7] S. Özcan, S. Tunali, T. Akar, A. Özcan, Biosorption of lead(II) ions onto waste biomass of *Phaseolus vulgaris* L.: Estimation of the equilibrium, kinetic and thermodynamic parameters, *Desalination* 244 (2009) 188–198.
- [8] T. Mohammadi, A. Razmi, M. Sadrzadeh, Effect of operating parameters on Pb<sup>2+</sup> separation from wastewater using electro-dialysis, *Desalination* 167 (2004) 379–385.
- [9] A. Abou-Shady, C. Peng, J. Almeria O, H. Xu, Effect of pH on separation of Pb (II) and NO<sub>3</sub><sup>-</sup> from aqueous solutions using electro-dialysis, *Desalination* 285 (2012) 46–53.
- [10] A.S. Ozcan, Ö. Gök, A. Özcan, Adsorption of lead(II) ions onto 8-hydroxy quinoline-immobilized bentonite, *J. Hazard. Mater.* 161 (2009) 499–509.
- [11] Z. Shi, F. Li, S. Yao, Adsorption behaviors of lead ion onto acetate modified activated carbon fiber, *Desalin. Water Treat.* 36 (2011) 164–170.
- [12] A.P.A. Salvado, L.B. Campanholi, J.M. Fonseca, C.R.T. Tarley, J. Caetano, D.C. Dragunski, Lead(II) adsorption by peach palm waste, *Desalin. Water Treat.* 48 (2012) 335–343.
- [13] M. Özacar, İ.A. Şengil, H. Türkmenler, Equilibrium and kinetic data, and adsorption mechanism for adsorption of lead onto valonia tannin resin, *Chem. Eng. J.* 143 (2008) 32–42.
- [14] F.M. Pang, P. Kumar, T.T. Teng, A.K.M. Omar, K.L. Wasewar, Removal of lead, zinc and iron by coagulation–flocculation, *J. Taiwan Inst. Chem. Eng.* 42 (2011) 809–815.
- [15] M. Tsunekawa, M. Ito, Y. Sasaki, T. Sasaki, N. Hiroyoshi, Removal of lead compounds from polyvinylchloride in electric wires and cables using cation-exchange resin, *J. Hazard. Mater.* 191 (2011) 388–392.
- [16] D. Kavak, M. Demir, B. Başsayel, A.S. Anagün, Factorial experimental design for optimizing the removal of lead ions from aqueous solutions by cation exchange resin, *Desalin. Water Treat.* 51 (2013) 1712–1719.
- [17] S. Ahmed, S. Chughtai, M.A. Keane, The removal of cadmium and lead from aqueous solution by ion exchange with Na-Y zeolite, *Sep. Purif. Technol.* 13 (1998) 57–64.
- [18] S.E. Kentish, G.W. Stevens, Innovations in separations technology for the recycling and re-use of liquid waste streams, *Chem. Eng. J.* 84 (2001) 149–159.
- [19] J.L. Cortina, N. Miralles, M. Aguilar, A.M. Sastre, Extraction studies of Zn(II), Cu(II) and Cd(II) with impregnated and Lewextrel resins containing di (2-ethylhexyl) phosphoric acid (Lewatit 1026 OC), *Hydrometall.* 36 (1994) 131–142.
- [20] Z.H. Huang, X. Zheng, W. Lv, M. Wang, Q.-H. Yang, F. Kang, Adsorption of Lead(II) Ions from aqueous solution on low-temperature exfoliated graphene nanosheets, *Langmuir* 27 (2011) 7558–7562.
- [21] E. Pehlivan, T. Altun, Ion-exchange of Pb<sup>2+</sup>, Cu<sup>2+</sup>, Zn<sup>2+</sup>, Cd<sup>2+</sup>, and Ni<sup>2+</sup> ions from aqueous solution by Lewatit CNP 80, *J. Hazard. Mater.* 140 (2007) 299–307.
- [22] S. Rengaraj, Y. Kyeong-Ho, M. Seung-Hyeon, Removal of chromium from water and wastewater by ion exchange resins, *J. Hazard. Mater.* B.87 (2001) 273–287.
- [23] A. Ohashi, T. Hashimoto, H. Imura, K. Ohashi, Cloud point extraction equilibrium of lanthanum(III), europium(III) and lutetium(III) using di(2-ethylhexyl)phosphoric acid and Triton X-100, *Talanta* 73 (2007) 893–898.
- [24] M. Benamor, Z. Bouariche, T. Belaid, M.T. Draa, Kinetic studies on cadmium ions by Amberlite XAD7 impregnated resins containing di(2-ethylhexyl) phosphoric acid as extractant, *Sep. Purif. Technol.* 59 (2008) 74–84.
- [25] B. Alyüz, S. Veli, Kinetics and equilibrium studies for the removal of nickel and zinc from aqueous solutions by ion exchange resins, *J. Hazard. Mater.* 167 (2009) 482–488.
- [26] M. Özacar, İ.A. Şengil, Two-stage batch sorber design using second-order kinetic model for the sorption of metal complex dyes onto pine sawdust, *Biochem. Eng. J.* 21 (2004) 39–45.
- [27] M. Horsfall, Jr, A.I. Spiiff, Effect of metal ion concentration on the biosorption of Pb<sup>2+</sup> and Cd<sup>2+</sup> by *Caladium bicolor* (wild cocoyam), *Afr. J. Biotechnol.* 4 (2005) 191–196.
- [28] Y.S. Ho, G. McKay, Pseudo-second order model for sorption processes, *Process Biochem.* 34 (1999) 451–465.
- [29] Y.S. Ho, Review of second-order models for adsorption systems, *J. Hazard. Mater.* B136 (2006) 681–689.
- [30] J.L. Cortina, R.A. Yellin, N. Miralles, A.M. Sastre, A. Warshawsky, Kinetics studies on heavy metal ions extraction by Amberlite XAD2 impregnated resins containing a bifunctional organophosphorous extractant, *React. Funct. Polym.* 38 (1998) 269–278.
- [31] N. Kabay, S. Sarp, M. Yuksel, O. Arar, M. Bryjak, Removal of boron from seawater by selective ion exchange resins, *React. Funct. Polym.* 67 (2007) 1643–1650.
- [32] R. Manski, H.J. Bart, W. Backer, J. Strube, M. Traving, A. Görg, Separation of cobalt and nickel by reactive extraction—modeling of equilibria, *Chem. Eng. Technol.* 29(12) (2006) 1513–1518.
- [33] S.H. Chang, T.T. Teng, N. Ismail, Efficiency, stoichiometry and structural studies of Cu(II) removal from aqueous solutions using di-2-ethylhexylphosphoric acid and tributylphosphate diluted in soybean oil, *Chem. Eng. J.* 166 (2011) 249–255.
- [34] D. Darvishi, D.F. Haghshenas, E.K. Alamdari, T.S.K. Sadrnezhaad, M. Halali, Synergistic effect of cyanex 272 and cyanex 302 on separation of cobalt and nickel by D2EHPA, *Hydrometall.* 77 (2005) 227–238.
- [35] B.S. Morais, M.B. Mansur, Characterisation of the reactive test system ZnSO<sub>4</sub>/D2EHPA in n-heptane, *Hydrometall.* 74 (2004) 11–18.